

Experimental Study of S-wave Propagation Through a Filled Rock Joint

Tingting Liu^{1,2} · Jianchun Li² · Haibo Li² · Xinping Li¹ · Yun Zheng² · Hui Liu¹

Received: 25 July 2016 / Accepted: 25 May 2017 / Published online: 15 June 2017
© Springer-Verlag Wien 2017

Abstract This experimental study proposes a Split Shear Plates model to investigate the effects of a filled joint on S-wave attenuation. A dynamic impact is used to create frictional slip and generate an incident S-wave. The filled joint is simulated using a sand layer between two rock plates. Normal stress is applied to the filled joint, and semiconductor strain gauges are arranged on the two plates to measure the strain. Verification tests are conducted to validate the reliability of the experimental results. A series of tests is performed to investigate the influence of the normal stress, filled thickness and particle size of the filling materials on the S-wave propagation. The transmission coefficients of the filled joints are smaller than those of the non-filled joints because of the attenuation associated with the filling materials. Additionally, the transmission coefficients exhibit a stronger correlation with the normal stress than with the filled thickness or particle size. The transmission coefficients increase at a decreasing rate as normal pressure increases.

Keywords Wave propagation · S-wave · Filled joint · Transmission coefficient · Normal stress

1 Introduction

Natural rock masses are often discontinuous because of the existence of fractures, joints and faults. Open joints are generally filled with clay, sand and rock debris. These filling materials may reduce the strength of the rock mass and affect the deformation behavior of the joints. Therefore, the filled joints are likely to be the weakest elements in a rock mass and control the shear behavior of the rock mass (De Toledo and De Freitas 1993; Indraratna et al. 2010; Barton 2013). When a wave propagates across a jointed rock mass, the presence of the joints not only induces wave amplitude attenuation but also decreases the wave propagation velocity. Therefore, the study of the wave propagation mechanisms of a filled joint is of great engineering significance to stability analyses of rock mass.

Based on the displacement discontinuity model (DDM), the influence of non-filled joints on wave propagation has been studied using theoretical analysis and numerical methods (Pyrak-Nolte et al. 1990; Zhao et al. 2006; Li 2013). However, few studies have analyzed the effects of filled joints on wave propagation, primarily because of the complexity of the multiple factors. Considering a filled joint as a thin layer, some researchers (Zhu et al. 2011; Li et al. 2013) have found that both the filled thickness and the properties of the filling material are significant for wave attenuation. In theoretical analysis, both non-filled and filled joints were simplified without considering various parameters such as the saturation state, the particle size of the filling material and the roughness of the joint wall. Thus, some experimental analyses were performed to study the interaction between the joints and wave propagation.

Four experimental methods are generally used to study wave propagation across a joint: the split Hopkinson pressure bar (SHPB) method, ultrasonic tests, resonant

✉ Tingting Liu
tliu@whut.edu.cn

¹ Key Laboratory of Roadway Bridge and Structure Engineering, Wuhan University of Technology, Wuhan 430070, Hubei, China

² State Key Laboratory of Geomechanics and Geotechnical Engineering, Institute of Rock and Soil Mechanics, Chinese Academy of Sciences, Wuhan 430071, Hubei, China

column apparatus (RCA) tests and earthquake wave or blast wave monitoring. The SHPB method is widely used to analyze longitudinal wave (P-wave) attenuation and the dynamic mechanical behaviors of samples. SHPB tests performed by Li and Ma (2009), Fan et al. (2012) and Wu et al. (2013) showed that the transmitted waves were affected by various factors such as the particle size, saturation state and thickness of the filling materials and the sedimentary characteristics of the rock.

Based on the relationships between the rock properties and the wave velocity, ultrasonic tests were conducted to investigate the effects of joint roughness, joint direction and joint number on wave propagation (Kahraman 2002; Zhao et al. 2006; Kurtuluş et al. 2012; Huang et al. 2014). In addition, RCAs and quasi-static resonant columns (QSRCs) have been used to investigate long-wavelength wave propagation across a joint by analyzing the P-wave velocity, S-wave velocity and damping ratio. RCA-based tests have been used to study the various factors that affect wave propagation, including normal stress and gouge (Fratta and Santamarina 2002), joint orientation (Sebastian and Sitharam 2015), rough 3D surfaces of naturally fractured rock (Mohd-Nordin et al. 2014) and roughness and joint spacing (Perino and Barla 2015).

When an earthquake occurs or when rock is excavated with explosives, the seismic/blast waves recorded at the site can be analyzed to understand the wave attenuation in a jointed rock mass. For example, Chopra et al. (2011) and Tripathi et al. (2014) studied the relationship between seismic wave attenuation and the quality factor. Hao et al. (2001) investigated the effects of joint angle on blasting-related shock wave propagation by analyzing motions recorded at different locations. These results revealed the dependence of the wave frequency and the joint direction on wave propagation.

However, previous experimental methods are not sufficient for the study of S-wave propagation. The SHPB method fails to consider S-wave propagation across a joint, and the amplitudes of ultrasonic waves are much smaller than those of seismic and blast waves. Moreover, RCA tests have mainly focused on the damping and wave amplitude attenuation of the whole sample, and the results from site records are influenced by both joints and a variety of complicated factors.

This paper proposes a new experimental apparatus for assessing S-wave propagation. A new device named the Split Shear Plates (SSP) apparatus is developed to investigate the effects of filled joints on S-wave propagation. Experimental tests are conducted to study the influence of the fill thickness, the particle size of the filling materials and the normal stress on the S-wave propagation.

2 Experimental Setup

2.1 Split Shear Plates Apparatus

The main difficulty associated with studying S-wave propagation in laboratory experiments is the generation of an S-wave. Wu and Zhao (2014) proposed a dynamic-induced direct shear model to investigate the dynamic triggering of frictional slip. In field tests of S-wave velocity, an S-wave is generated from the dynamic friction between a heavy weight and the ground by striking the weight with a hammer. Next, the S-wave velocity is attained based on the time interval and corresponding distance. The Split Shear Plates (SSP) apparatus is designed based on frictional slip and basic SHPB theory. The plan view of the test apparatus is shown in Fig. 1a, b. The SSP apparatus consists of two rock plates (i.e., the incident plate and the transmitted plate), a normal load setup, a friction bar made of stainless steel and a dynamic triggering system.

Both the incident plate and the transmitted plate are granite rock plates. The two granite rock plates are closely examined to ensure homogeneity, compactness and the existence of few visible fractures. Young's modulus and shear modulus of the granite plate are 47.3 and 31.5 GPa, respectively. The density is 2850 kg/m³ and the S-wave velocity is 3324 m/s. The thickness and width of each plate are 30 and 300 mm, respectively. The lengths of the incident plate and the transmitted plate are 670 and 630 mm, respectively. The incident plate and the transmitted plate are placed on two stainless steel plates to reduce the friction effects of the supports. Each stainless steel plate is welded to two rollers, which are set on a track to control movement in the direction perpendicular to the wave propagation. The steel plate is 60 mm long, 200 mm wide and 30 mm thick.

Normal load is applied using a hydraulic pump at the end of the transmitted plate. The normal stress is held constant during the experiment and the maximum stress reaches 10 MPa. A piece of highly flexible rubber is placed between the transmitted plate and the normal load to uniformly distribute the normal stress.

2.2 The Dynamic Triggering System

The dynamic triggering system is composed of a roller support, a bullet, a compression spring and a controlled bar (Fig. 1b). Two compressed springs with a stiffness coefficient of 10 N/mm are used to generate pulse loading, which can be changed by adjusting the compressed lengths of the springs. The springs are controlled by a controller bar and can be released instantaneously. The friction bar is a

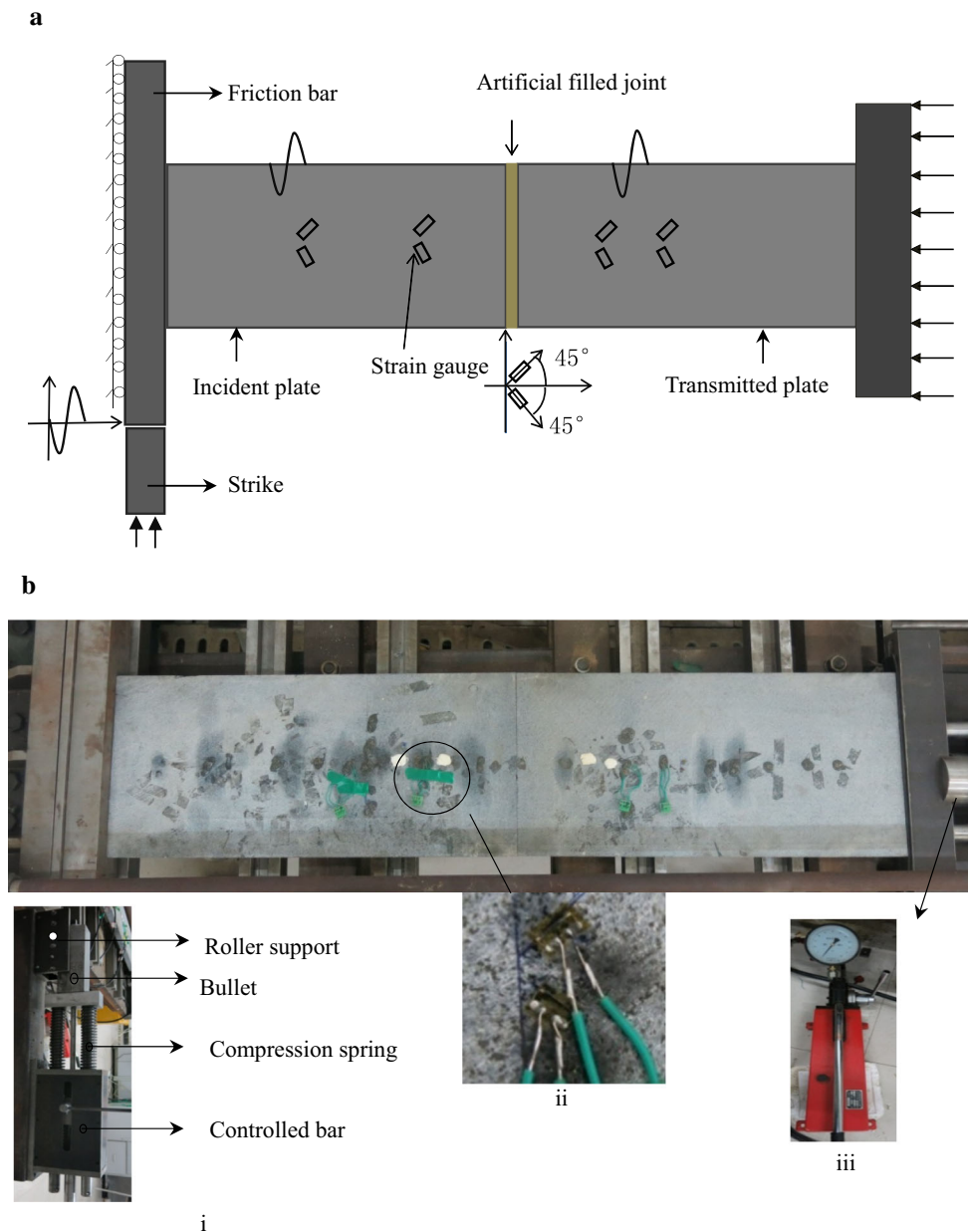


Fig. 1 Split Shear Plates model. **a** Schematic diagram of the design principle and **b** the plan form of the test apparatus: (i) the dynamic loading device, (ii) semiconductor gauge and (iii) normal stress loading device

cuboid with dimensions of 10 mm × 10 mm × 600 mm. The rolling friction coefficient of the roller support of the frictional bar is approximately 0.001, whereas the friction coefficient of interface 1 between the frictional bar and the incident plate is larger than 0.3. For a normal load of up to 20 kN, the maximum frictional force from the roller support is approximately 20 N, whereas that of interface 1 is larger than 6 kN. Thus, the friction force from the roller support of the frictional bar can be neglected because the rolling friction is much smaller than that generated by interface 1.

Similar to field tests of the S-wave velocity, an S-wave is generated using dynamic friction between a friction bar and the incident plate. The dynamic slip of the friction bar is induced by an impact event between a bullet and the front end of the friction bar. This impact creates dynamic friction at the interface between the incident plate and the friction bar. The left side and the underside of the friction bar are smooth planes, and the friction effect of the supports is eliminated by a pair of rollers. However, the right side of the friction bar, which is the surface in contact with the incident plate, is roughened to increase the friction.

2.3 Measurement and Acquisition

The incident wave and transmitted wave are measured by strain gauges located on the incident plate and transmitted plate, respectively. Normal strains cause dimensional changes in a strain gauge grid, changing its electrical resistance. However, a strain gauge does not directly respond to shear strain because shear strain merely rotates the grid. Based on the laws of elasticity, shear strain can be calculated from the normal strain and the angles of two strain gauges. When the gauge axes of a two-gauge 90° rosette are aligned with the principal axes, the half-bridge strain gauge measurement in a Wheatstone bridge circuit is numerically equal to the shear strain (Perry 1969). Thus, the shear strain waves are measured using a pair of strain gauges located at 45° angles to the direction of S-wave propagation [Fig. 1b(ii)].

Moreover, conventional strain gauge cannot be used in this experiment because the shear strain signals generated by the dynamic friction are smaller than 20 $\mu\epsilon$. Thus, semiconductor strain gauges with high sensitivity are used to measure the incident wave and the transmitted wave. The sensitivity coefficient of the semiconductor strain gauges is 100, which is approximately 50 times higher than that of a resistive strain gauge. In addition, a dynamic strain indicator and an oscilloscope are used to record the strain time with a sampling rate of 10⁵ Hz.

3 Verification Experiment

This study focuses on the influence of filled joints on a normally propagating S-wave by assuming the S-wave to be a one-dimensional wave. The deformation of a joint filled with a thin sand layer is considered homogeneous, and the S-wave in this study is a plane wave; thus, the waveforms recorded at the same wave front are approximately the same. Consequently, strain gauges IS1, IS2, IS3 and IS4 are glued to the incident plate, and strain gauges TS1, TS2 and TS3 are glued to the transmitted plate perpendicular to the wave propagation direction at the same wave front, as shown in Fig. 2. The strain gauges are placed away from the edge of the plate to eliminate concentrated stress effects.

When a wave propagates through a rock mass, energy may be absorbed by the internal pores and micro-cracks in the mass. This attenuation induced by the rock plate itself may cause errors when analyzing the effects of the filled joints. Therefore, four strain gauges, named A, B, C and D, are positioned at the center of the plate in the direction of wave propagation to determine whether attenuation is caused by only the filled joint. Because the granite plates used in this experiment are not very long, the incident pulse

and the reflection pulse may overlap, inducing inaccurate calculations such as wave amplitude and frequency. Thus, based on one-dimensional wave propagation theory, the wave separation method is adopted to obtain the incident wave and reflection wave before verifying the wave attenuation.

3.1 Plane Wave Verification

The strain–time responses recorded by strain gauges IS1–IS4 at different positions are nearly identical, as shown in Fig. 3. Although there are some differences, the head waves of the four sets of strain gauges IS1–IS4 approximately formed a series of half-sinusoidal waves with a frequency of 6 kHz. The waveforms became irregular after that time. This phenomenon might be caused by the superposition of the incident and reflection P-waves in the friction bar or vibration of the support. Although a P-wave is generated in the friction bar, the S-wave generated by the dynamic slip is the focus of this study. This study mainly focuses on methods of laboratory testing the S-wave and the attenuation of the S-wave. The stress caused by the secondary waves appears to be complicated and has not been considered (Wu et al. 2013). The strain–time responses recorded by strain gauges TS1–TS3 are not sinusoidal waves. However, the amplitude and frequency are almost identical. It should be noted that the incident wave and the transmitted wave are not accurate plane waves because the S-wave is scattered along the two interfaces. Therefore, the shear strain is inhomogeneous along the interfaces. This inhomogeneity would gradually become smaller with the wave propagation along the incident plate and the transmitted plate. The farther away from the two interfaces, the smaller the inhomogeneity and the closer to the plane wave; thus, the waves in the middle of the plate are approximated and considered as plane waves.

3.2 Wave Separation

Zhao and Gary (1997) presented a two-gauge measurement method for correcting wave dispersion effects. Wave propagation was analyzed using the SHPB method with different pressure bar materials based on the wave separation method (Meng and Li 2003; Li and Ma 2009; Wu et al. 2013). It should be noted that the wave velocity in the present calculation is the S-wave velocity rather than the P-wave velocity. Based on the theories presented in previous studies, wave separation using two-point measurements of strain and particle velocity is described in detail. The distance between strain gauges M1 and M2 is assumed to be l_0 , and the strains directly recorded by these gauges are ϵ_{m1} and ϵ_{m2} , respectively. These variables represent the strain

Fig. 2 Schematic diagram of the strain gauge locations in the verification experiment

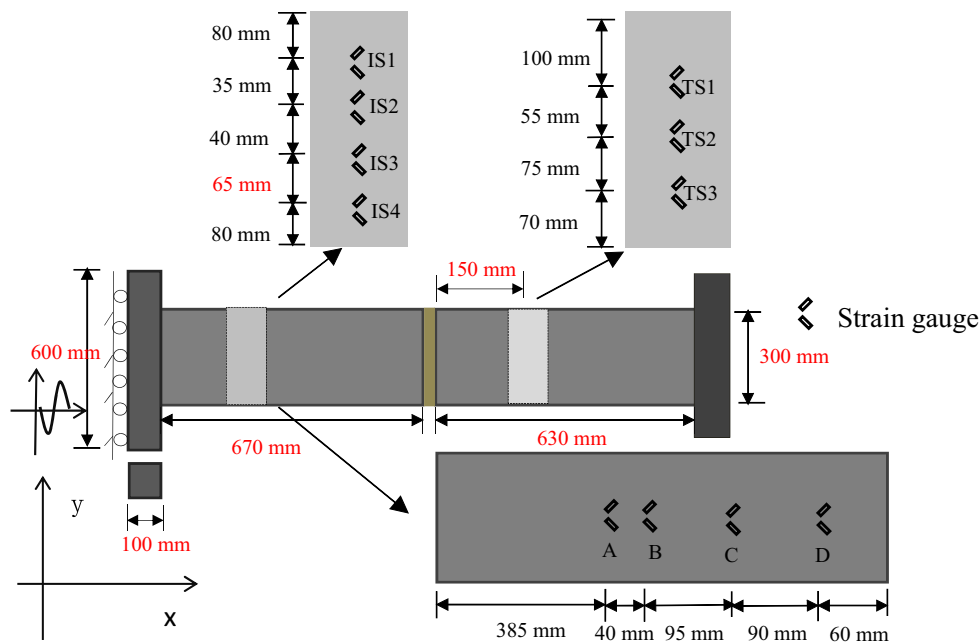
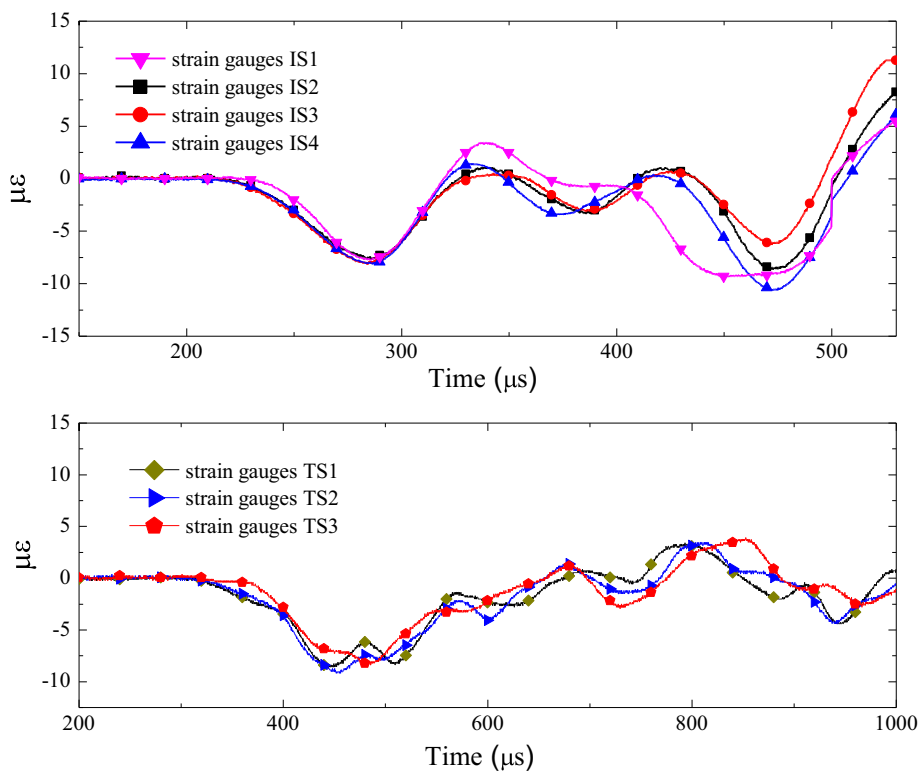


Fig. 3 Verification tests results for the plane S-wave



superposition of the incident and reflection waves, which are denoted by ϵ_{m1}^I and $\epsilon_{m1}^R(t)$ for gauge M1 and by ϵ_{m2}^I and $\epsilon_{m2}^R(t)$ for strain gauge M2, respectively. These variables can be separated and expressed using a time-shifting function:

$$\begin{aligned} \epsilon_{m1}^I(t) &= \epsilon_{m1}(t) - \epsilon_{m1}^R(t) & \epsilon_{m1}^R(t) &= \epsilon_{m2}^R(t - \Delta t) \\ \epsilon_{m2}^I(t) &= \epsilon_{m1}^I(t - \Delta t) & \epsilon_{m2}^R(t) &= \epsilon_{m2}(t) - \epsilon_{m2}^I(t) \end{aligned} \quad (1)$$

where $\Delta t = l_0/c_s$ is the time interval between strain gauges M1 and M2. Therefore, wave separation is performed by

analyzing the measurements of strains gauges B and C or strains gauges B and D.

The incident waves, reflection waves and original measurements recorded by strain gauges B, C and D are shown in Fig. 4. The approximate half-sinusoidal incident wave after wave separation is the same as the initial measurement at gauge B, i.e., the superposition of the primary part of the wave recorded by gauge B can be neglected. However, the differences between the descending portions of the incident waves and the initial measurements of strain gauges C and D are more apparent; therefore, superposition occurs and should be considered at strain gauges C and D.

The primary part of the measurement recorded by strain gauge B can be considered the incident wave, and it is used in the following analysis. Wave separation does not need to be performed for the transmitted wave because the distance between strain gauge TS2 and the end of the transmitted plate is sufficiently large.

3.3 Wave Attenuation of the Rock Plate

Verification tests of strain gauges A, B, C and D are performed to investigate the effects of the inner pores and micro-cracks of the rock plate on wave attenuation. As shown in Fig. 5, the primary parts of the original waves recorded by strain gauges A, B and C in different positions are similar. The strain–time response recorded by strain gauge D differs from the measurements of the other three

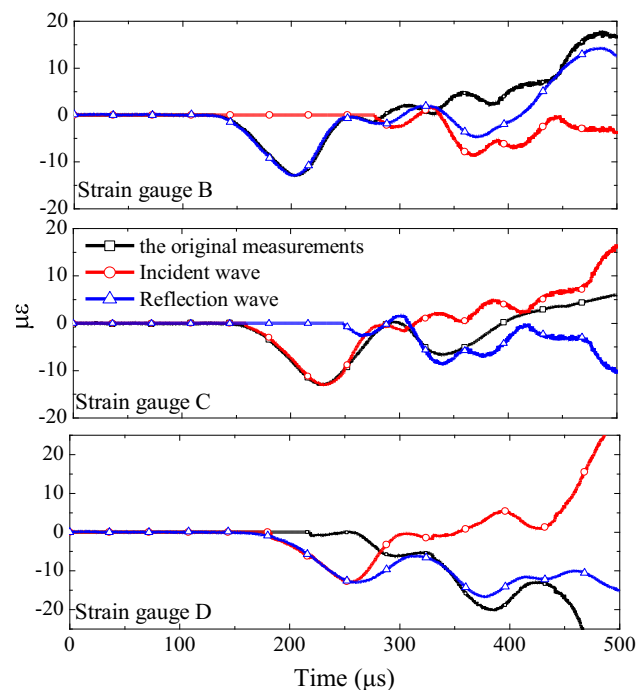


Fig. 4 Wave separation results based on the strain gauge locations

because of the short distance between strain gauge D and the edge of the incident plate, where the incident and reflection waves overlap. The similar incident waves of the four strain gauges after wave separation further verify this conclusion. The analogous waveform and amplitude indicate that attenuation and distortion can be neglected for the S-wave propagation.

4 SSP Tests and Results

This study investigates the role that filled joints play in S-wave propagation, and tests of non-filled joints are performed for comparison. River sand formed through the interactions of water and natural stones is used in the experiment. The main component of the river sand is silica, which contains a small amount of mica. Sand layer thicknesses of 3, 4 and 5 mm are used to investigate the influence of filled joint thickness on wave attenuation. Furthermore, as shown in Fig. 6, two sand layers with different particle sizes, 0.075–0.25 mm and 0.5–1.0 mm, are used to simulate different filling materials. The two surfaces of the joint, used as end planes of the incident plate and the transmitted plate, are processed using a cutting machine. The joint walls are smooth planes without apparent roughness. Barton and Choubey (1977) proposed a parameter, the joint roughness coefficient (JRC), to describe the joint wall asperity. Based on the back analysis of the conventional shear box tests, the JRC in this study is approximately 0.4, indicating that the joint can be seen as a smooth plane joint.

An oil pump is used to control the normal load. To eliminate the errors induced by Jack piston friction and oil path length, calibration tests are conducted to obtain the relationship between the actual normal load F_n (unit: kN) and the pressure gauge reading σ_r (unit: MPa). The calibration curve is shown in Fig. 7, and the relationship between F_n and σ_r can be expressed as follows:

$$\sigma_r = -0.4 + 0.20173F_n \quad (2)$$

The width and the thickness of the incident plate and the transmitted plate are 300 and 30 mm, respectively. The normal stress on the two plates can be converted as follows:

$$\begin{aligned} \sigma &= F_n / (0.3 \times 0.03) / 10^3 = (4.957\sigma_r + 0.1983) / 0.009 \\ &= 0.55\sigma_r + 0.022 \end{aligned} \quad (3)$$

Thus, for a given thickness and particle size of the sand layer, the normal stresses on the sand layer can be calculated using Eq. (2). In particular, the normal stresses applied to the sand layer are 0.6, 1.1, 1.6 and 2.2 MPa when the hydraulic pump produce loads of 1, 2, 3 and

Fig. 5 Verification test results for wave attenuation caused by the rock plate

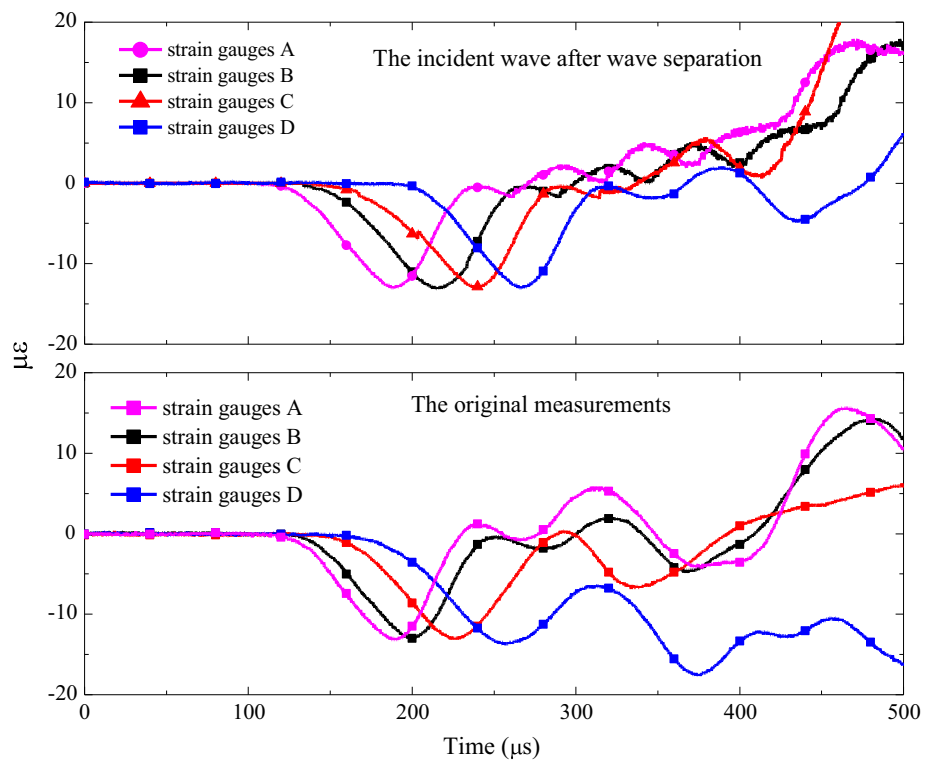
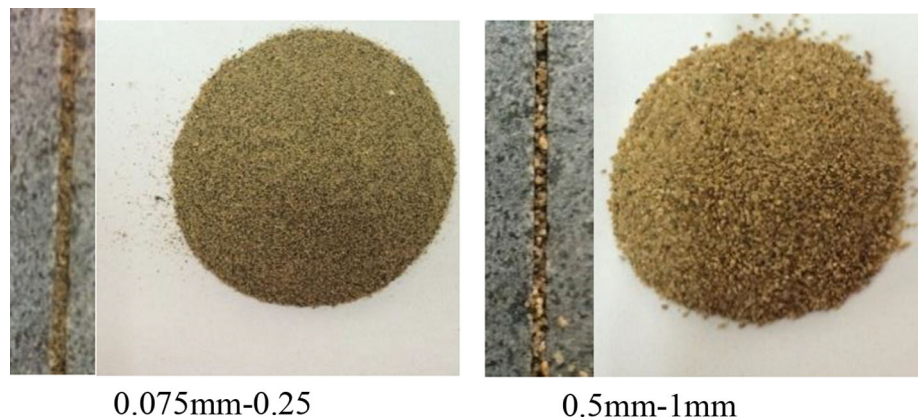


Fig. 6 Filling materials and sample photographs of the two particle sizes



4 MPa, respectively, in this experiment. The interfaces between the two granite bars are smooth and exhibit solid contact. Overall, 32 groups of tests are performed.

4.1 Effects of Normal Stress on the Waveform

As an important characteristic of geotechnical engineering such as high slope and deep underground construction, crustal stress affects not only the mechanical behavior of rock blocks but also the mechanical properties of the rock joints, such as the shear strength and the shear deformation characteristics. Consequently, normal stress is applied in the tests to simulate the influence of crustal stress on S-wave propagation.

In the SSP model, two interfaces are affected by the normal stress, σ_n . One is the contact surface between the friction bar and the incident plate, which is used to generate the S-wave. The other is interface 2 between the incident plate and the transmitted plate, which is treated as the joint wall. If no filling materials are used, the incident plate and transmitted plate make direct contact. In this case, the interface is considered a non-filled joint plane with an insignificant surface profile.

Increasing normal stress increases the friction at the interface and induces a large release of shear strain energy under external perturbations, i.e., the amplitudes of the incident S-wave and the transmitted wave increase as the normal stress increases. As shown in Fig. 8, when the

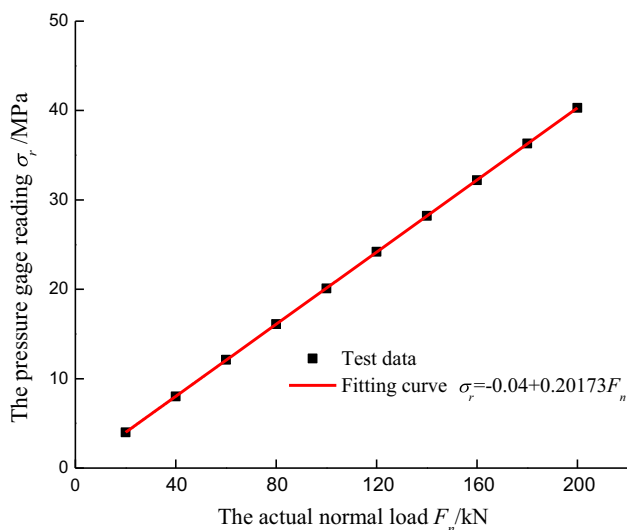


Fig. 7 Calibration curve of the oil pump

normal stresses increase from 0.6 to 2.2 MPa, the amplitudes of the incident wave increase from 4.2 to 16.3 μe for the non-filled joint and from 3.2 to 15.7 μe for the filled joint. For transmitted waves, the amplitude increases from 1.7 to 14.3 μe for the non-filled joint and from 0.8 to 8.5 μe for the filled joint. The amplitudes of the transmitted wave increase approximately tenfold as the normal stress increases. The amplitude increase in the transmitted wave is much larger than that of the incident wave, suggesting that increasing normal stress increases the S-wave transmission.

For the non-filled joint, increasing the normal stress increases the contact stress at the interface between the two rock walls, increasing both the friction force and the shear stiffness. For the filled joint, the normal stress not only changes the contact stress at the interface between the rock and the filling materials but also affects the shear mechanical behavior of the filling materials by increasing the compactness of the filling materials and decreasing the porosity of the granular matrix. These results suggest that the effect of the crustal stress on S-wave propagation cannot be neglected.

4.2 Effects of Normal Stress on the Transmission Coefficient

The transmission coefficient T is defined as the ratio of the amplitude of the primary parts of the transmitted wave to that of the incident wave. The transmission coefficients, T , for filled joints with two different filling materials and a non-filled joint are shown in Fig. 10. The experiment results indicate that T increases as σ increases, which is attributed to the constraint effect of σ on the attenuation. T increases nonlinearly with increased σ . However, the

increment rate gradually decreases. For example, as σ increases from 0.6 to 1.1 MPa, T increases by approximately 102% for the filled joint with a thickness of 3 mm and by 46.7% for the non-filled joint. However, when σ increases from 1.6 to 2.2 MPa, T increases by 12.8% for the filled joint with a thickness of 3 mm and by 10.7% for the non-filled joint. Accordingly, the relationship between T and σ is regressed using the following hyperbolic function:

$$T = A_1 \sigma_n / (A_2 + \sigma_n) \quad (4)$$

where A_1 and A_2 are the curve-fitting coefficients. The values of these coefficients are given in Table 1 for different cases. A peak T value may exist for each case as σ increases, and this peak value is equal to A_1 when σ is sufficiently high. In other words, for S-wave propagation, a filled joint may reach an upper limit under extremely high normal stress. For a non-filled joint, the value of A_1 is 1.08. This value does not suggest that the amplitude of the transmitted wave is larger than that of the incident wave; however, it implies that the influence of the non-filled joint on wave propagation may decrease at a high normal stress. The values of T for the filled joints are approximately 35.6–54.5% smaller than those of the non-filled joint. The A_1 of filled joints are approximately 9.3–44.5% smaller than those of non-filled joints, confirming the larger attenuation of filling materials.

4.3 Effects of the Filled Thickness

The amplitudes of the transmitted waves are much smaller for the filled joint than for the non-filled joint, although no apparent discrepancy is shown between the incident wave amplitudes for the filled joint and non-filled joint, as shown in Fig. 9. In addition, the jump time t_j , which is the critical time of the strain changed from 0. The t_j of the transmitted waves for the filled joint is later than that of the non-filled joint, suggesting that the filling material delays S-wave propagation. The filling materials exert two main influences on wave propagation. First, filling materials change the contact status of the joint, generally decreasing the friction angle and the shear stiffness of the joint and enhancing the attenuation of the S-wave. Second, the filling materials increase the propagation time. For the filled joint, the shear mechanical behavior of the filling materials is important for wave propagation. The slip failure of the filled joint may occur internally in the filling materials or at the interfaces between the filling materials and the rock wall. The results demonstrate both that the filled joints absorbed more energy and that rock masses with filled joints have poor stability (Fig. 10).

As one of the characteristic parameters of a filled joint, filled thickness is important for determining the mechanical

Fig. 8 Incident shear strain waves and transmitted shear strain waves under different normal stresses (σ_n) in a **a** non-filled joint and **b** filled joint ($h = 3$ mm, coarse particle)

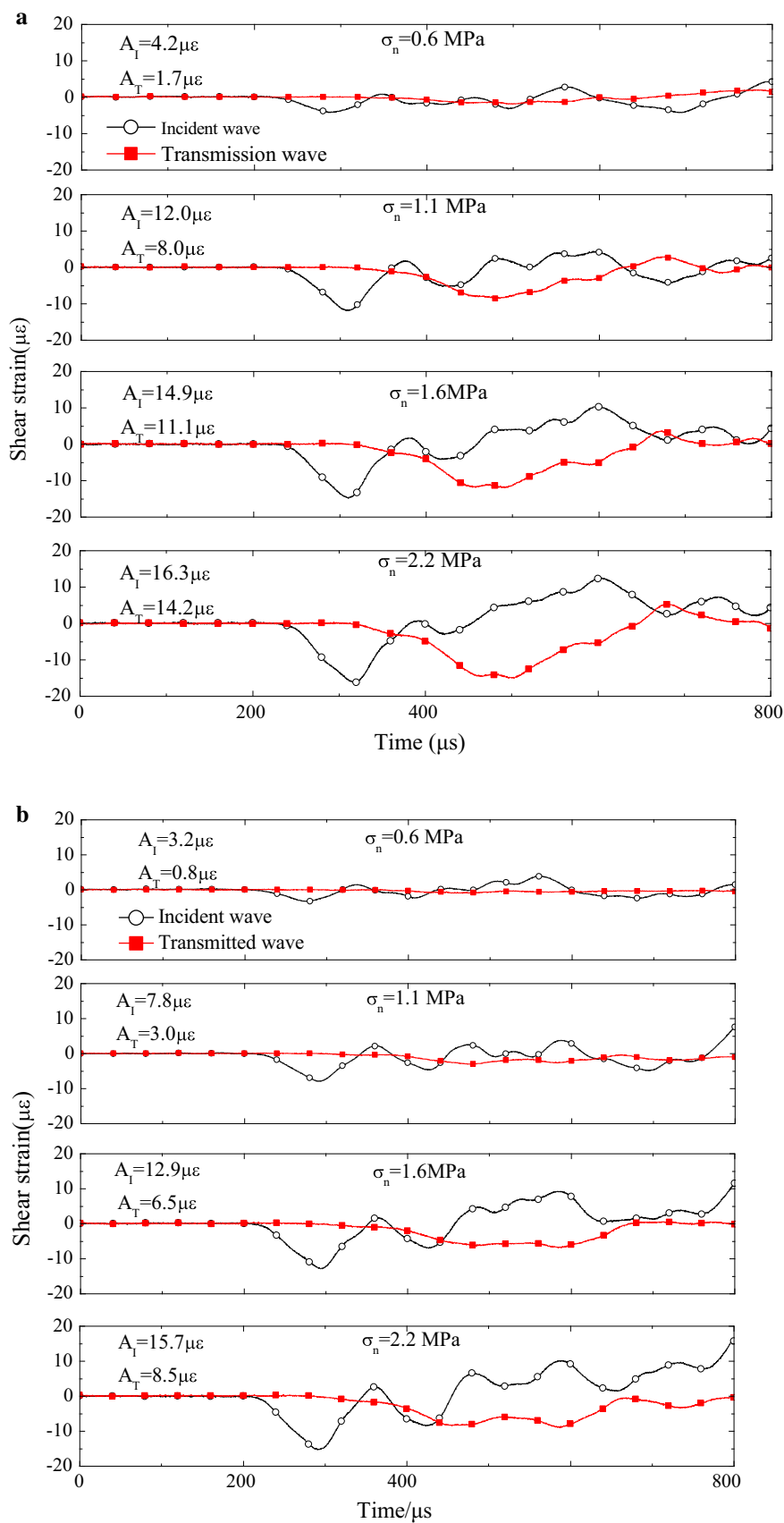
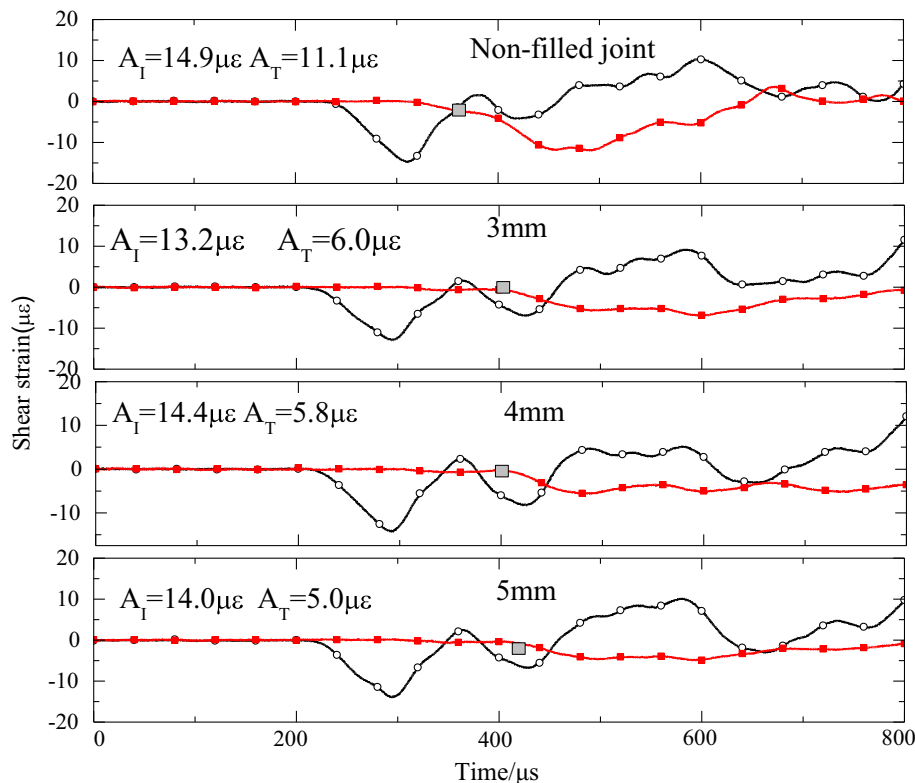


Table 1 Values of curve-fitting coefficients for different cases

Curve-fitting coefficients	Non-filled	Fine particle			Coarse particle		
		3 mm	4 mm	5 mm	3 mm	4 mm	5 mm
A_1	1.08	0.98	0.79	0.78	0.67	0.64	0.6
A_2	0.89	2.52	1.81	1.84	0.98	1.4	1.5

Fig. 9 Incident and transmitted waveforms with various filled thicknesses

behavior of a filled joint. For the filled joints in this experiment, the waveforms are similar at different fill thicknesses. For $\sigma_n = 1.6$ MPa and fine particles, the amplitudes of the transmitted waves decrease from 6 to 5.0 $\mu\epsilon$ as the fill thickness increases from 3 to 5 mm. The results indicate that thicker fills result in greater absorption of energy and more severe wave attenuation. Li (2013) and Li et al. (2013) found that as the fill thickness increased from 3 to 5 mm, the transmission coefficients of P-wave propagation decreased by almost 100%. In this study, under the same normal stress, the max value of T decreases by less than 50% as the fill thickness increases, as shown in Fig. 11. One reason for the smaller effect of filled thickness is that the filled joint in the experiment featured planar walls and therefore did not consider asperities or roughness. In addition, the influence of thickness on S-wave propagation is weaker than that on P-wave propagation because the propagation direction of the wave is different. The force direction is along the material thickness when one-dimensional P-wave propagation occurs across the

filled joint, whereas the stress direction of the S-wave is perpendicular to the direction of the fill thickness.

4.4 Effects of the Particle Size

The particle size of the filling materials is also a characteristic parameter of a filled joint, and existing studies of wave attenuation across filled joints have not considered its effect. The particle size not only significantly affects the physical characteristics (such as wave velocity, porosity and density) of the filling material but also affects the shear mechanical behavior (such as the frictional angle and the shear strength) of the filling material. In addition, particle size has important effects on the contact characteristics of the interface between the rock wall and the fill, such as the contact area and the frictional force. The relationship between the fill thickness and different normal stresses for two particle sizes is shown in Fig. 11. The transmission coefficients of the coarse particles are slightly smaller than those of the fine particles, especially at larger normal

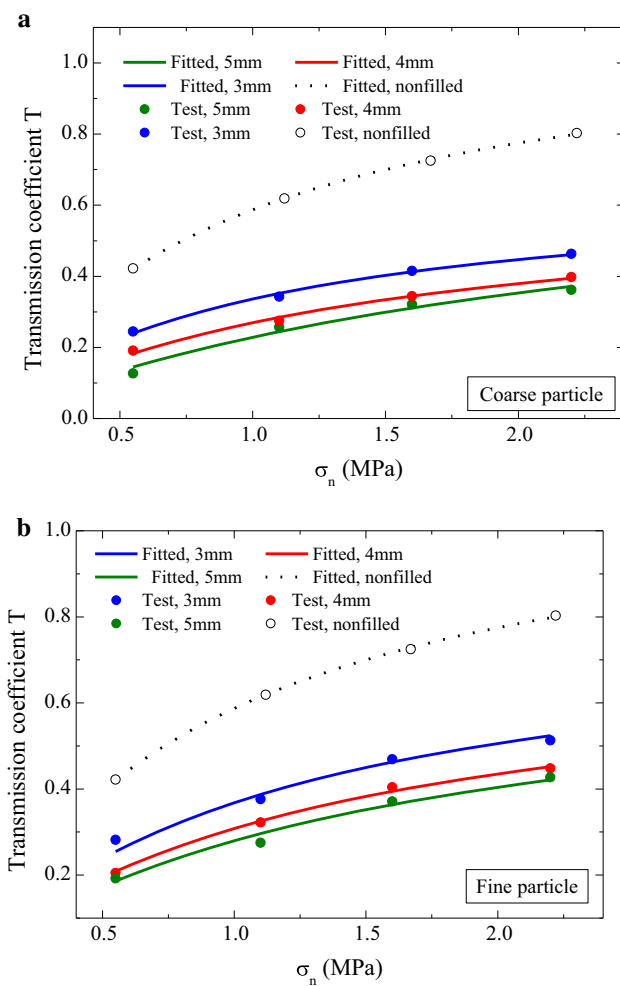


Fig. 10 Effect of filled thickness on the transmission coefficient under different normal stresses **a** coarse particle and **b** fine particle

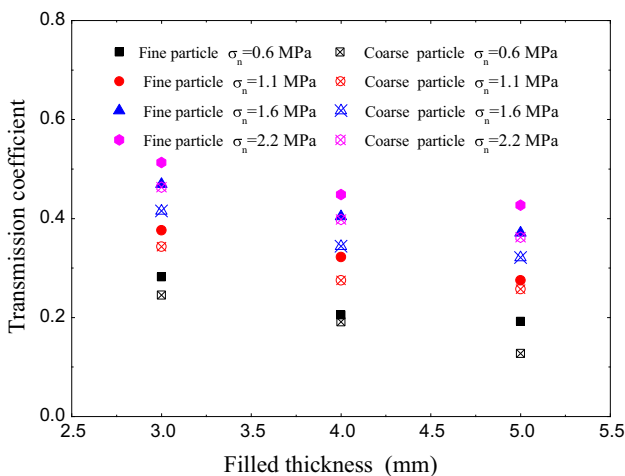


Fig. 11 Effect of particle size on the transmission coefficient under different normal stresses

stresses. The values shown in Table 1 also illustrate that the values of A_I are larger for fine particles; thus, the attenuation of the S-wave across a joint filled with coarse particles is greater than that across a joint filled with fine particles. This phenomenon maybe explained as follows.

Coarse particles with strong contacts can form a skeleton for wave propagation, whereas fine particles can easily flow and consume much more energy. It seems that more attenuation should have occurred when a wave propagates across a joint filled with fine particles, which seems to conflict with the test results. However, the porosity of coarse particles is larger than that of fine particles, and the contact area between coarse particles and rock walls is smaller. These features result in the occurrence of more attenuation in the joint filled with coarse particles, as shown in Fig. 11. Moreover, fine particles are more likely to undergo compression associated with the production of a certain amount of cohesive strength, further promoting the propagation of stress waves. This result is also consistent with the conclusion drawn by Gui et al. (2016).

5 Conclusions

This study introduces the SSP model to investigate the effects of normal stress, fill thickness and the particle size of filling materials on S-wave propagation. The SSP model has some limitations. For example, the amplitude of the incident wave is too small to induce failure of the filled joint, and the secondary wave behind the primary part of the wave is not taken into account. Moreover, the incident wave and the transmitted wave are not accurate plane waves. Despite these limitations, the SSP model provides a possible solution to investigate S-wave propagation across a filled joint or an unfilled joint using laboratory tests. In addition, the effects of normal stress can be considered. Conclusions from this study can be drawn as follows:

1. The incident waveforms are an approximate series of half-sinusoidal waves. For a given normal stress, the transmission coefficients of the filled joints are 9.3–44.5% smaller than those of the non-filled joints, illustrating the strong attenuation effect of the filling materials and verifying the negative effect of filled joints on the rock mass stability.
2. In natural rock masses, crustal stress is a geological condition that is important for wave attenuation. In the SSP model, crustal stress is simulated as normal stress. The increasing normal stress increases the contact stress of the two interfaces for no filled joint, increasing both the friction force and the shear

stiffness. For the filled joint, the normal stress not only changes the contact stress but also affects the shear mechanical behavior of the filling materials by compacting the filling materials.

3. As the normal stress increases, the amplitudes of the incident wave and transmitted wave increase, and the transmission coefficients increase nonlinearly. A hyperbolic expression can be derived to describe the relationship between the transmission coefficient and the normal stress. Moreover, the transmission coefficient may have an upper limit when the normal stress is sufficiently large. For a filled joint, the upper limit is related to the fill thickness and the particle size. For a non-filled joint, the upper limit is close to 1, suggesting that S-wave transmission in a non-filled joint may decrease when the normal stress is sufficiently large.
4. The transmission coefficient decreases slightly when increasing fill thickness for a given normal stress and filling materials. For a plane-filled joint, the effect of the fill thickness on S-wave propagation is not as obvious as that on P-wave propagation because the S-wave propagation direction is perpendicular to the fill thickness direction.
5. For a given normal stress and fill thickness, the transmission coefficients of the coarse particles are slightly smaller than those of fine particles. This difference is greater under large normal stresses because the coarse particles have greater porosity and smaller contact area between the filling materials and rock wall. Moreover, under high normal stress, fine particles may be compressed and produce a certain amount of cohesive strength.

Although there are some limitations to this study, an S-wave under normal stress can be observed and analyzed. The experiment setup can be modified to further investigate S-wave propagation through a single filled joint or a set of filled joints with different asperities.

Acknowledgements The authors acknowledge the anonymous reviewers and the editor for their valuable comments and suggestions. This paper has received financial support from the National Natural Science Foundation of China (Grant Nos. 41525009, 51609183) and the Open Research Fund of the State Key Laboratory of Geomechanics and Geotechnical Engineering, Institute of Rock and Soil Mechanics, Chinese Academy of Sciences (Grant No. Z015005).

References

- Barton N (2013) Shear strength criteria for rock, rock joints, rockfill and rock masses: problems and some solutions. *J Rock Mech Geotech Eng* 5:249–261. doi:10.1016/j.jrmge.2013.05.008
- Barton N, Choubey V (1977) The shear strength of rock joints in theory and practice. *Rock Mech Rock Eng* 10:1–54

- Chopra S, Kumar D, Rastogi BK (2011) Attenuation of high frequency P and S waves in the Gujarat region, India. *Pure Appl Geophys* 168:797–813. doi:10.1007/s00024-010-0143-8
- De Toledo PE, De Freitas MH (1993) Laboratory testing and parameters controlling the shear strength of filled rock joints. *Geotechnique* 43:1–19. doi:10.1680/geot.1993.43.1.1
- Fan LF, Ren F, Ma GW (2012) Experimental study on viscoelastic behavior of sedimentary rock under dynamic loading. *Rock Mech Rock Eng* 45:433–438. doi:10.1007/s00603-011-0197-7
- Fratta D, Santamarina JC (2002) Shear wave propagation in jointed rock: state of stress. *Geotechnique* 52:495–505. doi:10.1680/geot.2002.52.7.495
- Gui YL, Zhao ZY, Zhou HY, Wu W (2016) Numerical simulation of P-wave propagation in rock mass with granular material-filled fractures using hybrid continuum-discrete element method. *Rock Mech Rock Eng* 49:4049–4060. doi:10.1007/s00603-016-0991-3
- Hao H, Wu Y, Ma G, Zhou Y (2001) Characteristics of surface ground motions induced by blasts in jointed rock mass. *Soil Dyn Earthq Eng* 21:85–98. doi:10.1016/S0267-7261(00)00104-4
- Huang X, Qi S, Guo S, Dong W (2014) Experimental study of ultrasonic waves propagating through a rock mass with a single joint and multiple parallel joints. *Rock Mech Rock Eng* 47:549–559. doi:10.1007/s00603-013-0399-2
- Indraratna B, Oliveira DAF, Brown ET (2010) A shear-displacement criterion for soil-infilled rock discontinuities. *Géotechnique* 60:623–633. doi:10.1680/geot.8.P.094
- Kahraman S (2002) The effects of fracture roughness on P-wave velocity. *Eng Geol* 63:347–350. doi:10.1016/S0013-7952(01)00089-8
- Kurtuluş C, Üçkardeş M, Sarı U, Güner ŞO (2012) Experimental studies in wave propagation across a jointed rock mass. *Bull Eng Geol Environ* 71:231–234
- Li JC (2013) Wave propagation across non-linear rock joints based on time-domain recursive method. *Geophys J Int* 193:970–985. doi:10.1093/gji/ggt020
- Li JC, Ma GW (2009) Experimental study of stress wave propagation across a filled rock joint. *Int J Rock Mech Min Sci* 46:471–478. doi:10.1016/j.ijmms.2008.11.006
- Li JC, Wu W, Li HB, Zhu JB, Zhao J (2013) A thin-layer interface model for wave propagation through filled rock joints. *J Appl Geophys* 91:31–38. doi:10.1016/j.jappgeo.2013.02.003
- Meng H, Li QM (2003) An SHPB set-up with reduced time-shift and pressure bar length. *Int J Implant Eng* 28:677–696. doi:10.1016/S0734-743X(02)00124-0
- Mohd-Nordin MM, Song K, Cho G, Mohamed Z (2014) Long-wavelength elastic wave propagation across naturally fractured rock masses. *Rock Mech Rock Eng* 47:561–573. doi:10.1007/s00603-013-0448-x
- Perino A, Barla G (2015) Resonant column apparatus tests on intact and jointed rock specimens with numerical modelling validation. *Rock Mech Rock Eng* 48:197–211. doi:10.1007/s00603-014-0564-2
- Perry CC (1969) Plane-shear measurement with strain gages. *Exp Mech* 9:19N–22N. doi:10.1007/BF02327879
- Pyrak-Nolte LJ, Myer LR, Cook NGW (1990) Anisotropy in seismic velocities and amplitudes from multiple parallel fractures. *J Geophys Res* 95:11345–11358. doi:10.1029/JB095iB07p11345
- Sebastian R, Sitharam TG (2015) Long wavelength propagation of elastic waves across frictional and filled rock joints with different orientations: experimental results. *Geotech Geol Eng* 33:923–934. doi:10.1007/s10706-015-9874-8
- Tripathi JN, Singh P, Sharma ML (2014) Attenuation of high-frequency P and S waves in Garhwal Himalaya, India. *Tectonophysics* 636:216–227. doi:10.1016/j.tecto.2014.08.015

- Wu W, Zhao J (2014) A dynamic-induced direct-shear model for dynamic triggering of frictional slip on simulated granular gouges. *Exp Mech* 54:605–613. doi:[10.1007/s11340-013-9823-5](https://doi.org/10.1007/s11340-013-9823-5)
- Wu W, Zhu JB, Zhao J (2013) Dynamic response of a rock fracture filled with viscoelastic materials. *Eng Geol* 160:1–7. doi:[10.1016/j.enggeo.2013.03.022](https://doi.org/10.1016/j.enggeo.2013.03.022)
- Zhao H, Gary G (1997) A new method for the separation of waves. Application to the SHPB technique for an unlimited duration of measurement. *J Mech Phys Solids* 45:1185–1202. doi:[10.1016/S0022-5096\(96\)00117-2](https://doi.org/10.1016/S0022-5096(96)00117-2)
- Zhao J, Cai JG, Zhao XB, Li HB (2006) Experimental study of ultrasonic wave attenuation across parallel fractures. *Geomech Geoeng* 1:87–103. doi:[10.1080/17486020600834613](https://doi.org/10.1080/17486020600834613)
- Zhu JB, Perino A, Zhao GF, Barla G, Li JC, Ma GW, Zhao J (2011) Seismic response of a single and a set of filled joints of viscoelastic deformational behaviour. *Geophys J Int* 186:1315–1330. doi:[10.1111/j.1365-246X.2011.05110.x](https://doi.org/10.1111/j.1365-246X.2011.05110.x)